ISSN: 0974-5823 Vol. 7 No. 1 January, 2022

International Journal of Mechanical Engineering

CFD Analysis for Heat Transfer Enhancement in Interfered Double Helical Heat Exchanger

Ghusoon Riadh Ibraheem,Ayser Muneer Flayh

Abstract

In the present work, two models of an interfered helical coil heat exchanger with two different diameters (1/2 and 5/8 inches) were designed and plotted by using ANSYS FLUENT R.18 to evaluate the performance of the heat exchanger. Flow rates of both cold and hot fluids were changed between 0.5 and 1.5 LPM, with temperature differences of 40 °C (K). For 0.5 inches diameter H.E., The maximum effectiveness andNTU value were 0.79 and 1.84,respectivelywhen applying 0.5 LPM cold water with 1.5 LPM hot water, while for 5/8 inches diameter H.E., The maximum effectiveness and NTU value were 0.696 and 1.36, respectivelywhen applying the same previous flow rates. Pitch decreasing from 31.756 mm (5/8 inches) to 25.4 mm (1/2 inches) causes effectiveness and NTUincreasing by approximately 15% and 35%, respectively.

Keyword:- Interfered double helical , heat transfer, pressure drop, CFD, heat exchanger.

1. Introduction

The obsession of diminishing cost, size and weight with improving the thermal performance of imitative heat exchangers, pushed the researchers to propose several heat transfer enhancement techniques. These techniques can be classified as passive methods and active methods **(Bergles et al., 1996)**. Passive methods do not need any direct application of external power, while the active techniques demand external power to be achieved. Generally, passive techniques utilizes surface and geometrical modifications applied on the flow channel such as rough surfaces , extended surfaces , displaced enhancement devices , swirl flow devices , curved (coiled) tubes , surface tension devices and use of additives. They promote higher heat transfer coefficient by disturbing or altering the existing flow behavior except for the extended surfaces**(Baqir et al., 2019)**. Curved tubes, and particularly coiled tubes, represent one of passive heat transfer enhancement techniques. This technique is very important because of the compact design of the coiled tubes, which demand smaller space, and the large heat transfer coefficient if compared with straight tubes. There are more various heat transfer applications which utilize curved tubes such as air conditioning and refrigeration systems, chemical reactors, food and dairy processes and heat recovery processes **(Ghobadi, 2014, Kong et al., 2018 and Ghashim and Flayh, 2020)**. When a fluid flow in a helical coiled tube, a secondary flow is produced due to the tube curvature, which results a secondary flow. So, the secondary flow has a very important effect on the difference in heat transfer and fluid flow characteristics between the helical coil and straight tubes **(Barua, 1963)**. In fact, secondary flow has a considerable capability to enhance heat transfer rate by making fluid in the middle of the coiled tube moving centrifugally outwards, and fluid near the wall inwards. This will lead to an augmentation in in NTU, exergy loss, and effectiveness.

(Mohanty, 2013)performed an analyzation for heat transferred through a helically coiled heat exchanger via ANSYS Fluent. This research attempted to analyze the influence of both counter and parallel flow on the heat rate completely transferred from a double helical heat exchanger, which consists of outer helical tube and inner helical tube. The researcher concludes that there was no high differences in heat transfer rate between parallel and counter flow arrangement. Pipes Nusselt number was varying between 340 and 360. Besides, the features of flow were investigated at constant temperature and constant heat flux. Velocity vector plot showed that fluid particles were subjected to an oscillatory motion inside the pipes. Pressure and temperature contours showed that the velocity and pressure values along the outer sides of the pipes were large if compared to the inner values. **(Bizhaem and Abbassi, 2017)** studied numerically laminar, developing flow of a nanofluid composed of Al_2O_3 and water with properties which depend on temperature in helical tube at constant wall temperature. They made a comparison for the numerical results with three test cases including nanofluid forced convection in straight tube, velocity profile in curved tube and Nusselt number in helical tubes. They noticed good agreement for all three cases. The researchers concluded that in entrance region, there is no thermal improvement provided by the nanofluid. They found also that better heat transfer enhancement and entropy generation reduction could be obtained at low Reynolds number. **(Datta et al., 2017)**performed a numerical investigation for a helical tube having laminar forced convection heat transfer with a heated wall. The researchers utilized direct numerical solution for 3-dimensional problem and compare the results with experimental results gained from **(Shatat, 2010)**. They achieved the investigation Prandtl numbers of values (4.02, 7.5 and 8.5). In the calculation of three dimensional model, with homogeneously heated wall temperature, they found the emergence of fully developed flow region. They found that Nusselt number gained from DNS method was in good coincidence with the experimental results for Pr = 0.85 which was gained from **(Shatat, 2010)** and also from **(Yang et al., 1995)** at low torsion when $\beta = 0.00012$. At the case of low torsion, Nusselt number decreases tenuously with the decreasing of Prandtl number, which gives a good coincidence with results gained from **(Yang et al., 1995)**. **(Sharifi et al., 2018)** used the CFD technique to study the coiled wire inserts effect on the friction coefficient, Nusselt number and overall efficiency in double pipe heat-exchangers. They found that when taking the benefit of suitable wire coils, the Nusselt values will be improved to 1.77 times. Besides, they suggested suitable friction coefficient and Nusselt number correlations for different coiled wire inserts with several geometry arrangements under the laminar flow. These two modified correlations could both be used for non-uniform helical wire insert geometries because their correlations were based on the occupied spaces where helical wires placed inside tubes.

So, many researchers have studied heat transfer enhancement in helical coiled heat exchangers by using various heat transfer enhancement techniques, which lead to positive results for some parameters and negative results for other parameters. In the present paper, heat transfer enhancement in an interfered coiled heat exchanger of a circular cross-section is studied numerically by using Ansys Fluent 18. The enhancement in heat transfer rate is expected due to the curvature of the flow which generates centrifugal force. Consequently, secondary flow or vortices are produced to promote higher heat transfer coefficients and result in comparatively more compact heat exchangers. A three dimensional simulation model of 7-turns interfered heat exchanger was established in detail numerical simulation by using CFD for the whole heat exchanger with different boundary conditions

.

Nomenclature

A_s	Surface Area, m^2	**Greek Symbols**	
C	Heat Capacity, J/s.K		
ρ	Density, Kg/m^3		
C_p	Specific Heat, J/ kg.K		
ε	Effectiveness		
D_C	Curvature Diameter, m	Δ	Difference

2. CFD Analysis

Computational fluid dynamics (CFD) study of the system is achieved bythe ANSYS Fluent R18 package.Firstly, a geometry of heat exchanger was drawing and then a suitable mesh up for it was building with setting the name selection for the parts of the system. Fluid and solid parts must be defined. System will be defined with more details in the set-up window to set the models, materials, cell zone conditions, boundary conditions and mesh interfaces. Finally, solution is initialized and calculations are run to obtain results which will be analyzed and discussed to have important conclusions.

2.1 Governing Equation

The modulated form of continuity, momentum and energy equations are as following **(Day, 2012)**:

Continuity Equation:

$$\frac{1}{r}\left\{\frac{\partial}{\partial x}(r\rho u)+\frac{\partial}{\partial r}(r\rho v)\right\}=0 \text{.....(1)}$$

X – Momentum Equation:

$$\frac{1}{r}\left\{\frac{\partial}{\partial x}(r\rho u^2)+\frac{\partial}{\partial r}(r\rho uv)\right\}=-\frac{\partial p}{\partial x}\pm\rho g+\left\{\frac{1}{r}\frac{\partial}{\partial r}\left(r\mu\frac{\partial u}{\partial r}\right)+\frac{\partial}{\partial x}\left(\mu\frac{\partial u}{\partial x}\right)\right\} \quad \text{..... (2)}$$

R - Momentum Equation:

$$\frac{1}{r}\left\{\frac{\partial}{\partial x}(r\rho uv)+\frac{\partial}{\partial r}(r\rho v^2)\right\}=-\frac{\partial p}{\partial r}+\left\{\frac{1}{r}\frac{\partial}{\partial r}\left(r\mu\frac{\partial v}{\partial r}\right)-\frac{v}{r^2}+\frac{\partial}{\partial x}\left(\mu\frac{\partial v}{\partial x}\right)\right\} \quad \text{..... (3)}$$

Energy Equation:

$$\rho c_p\left\{u\frac{\partial T}{\partial x}+v\frac{\partial T}{\partial r}\right\}=\frac{\partial}{\partial x}\left(\lambda\frac{\partial T}{\partial x}\right)+\frac{1}{r}\frac{\partial u}{\partial r}\left(\lambda\frac{\partial T}{\partial r}\right) \quad \text{.....(4)}$$

2.2 Geometry

Heat exchanger is drawn by ANSYS FLUENT workbench design modular as shown in figure (1). It is consists of two interfered 7-turns helical pipes, one for the cold fluid and the other for the hot fluid. The two pipes are touched together directly so there is no air gap between the turns of the heat exchanger. For

the purpose of increasing the conduction area, a thin sheet of copper was fixed as a pad inside the heat exchanger. So, the geometry was drawn as five parts, two solid parts and two fluid parts (which fill the solid parts) with additional part represent the copper sheet. The simulation was performed twice for two pipes diameters; ½ inches and 5/8 inches. The dimensions of the two helical heat exchangers are tabled below in table (1)

.

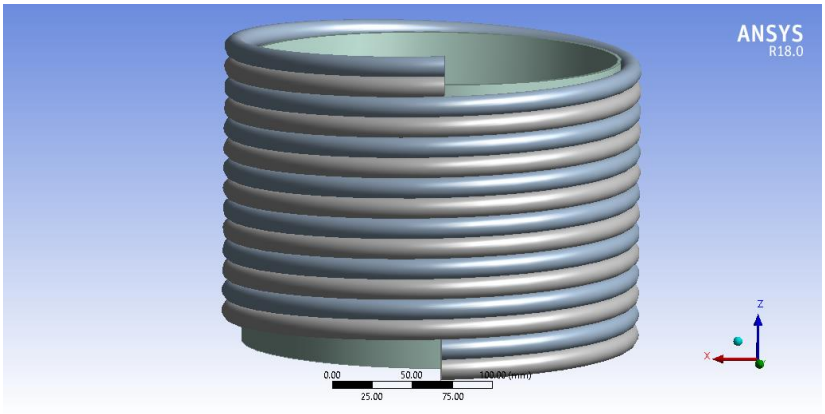

Figure (1) Interfered Helical Heat Exchanger

Table (1) Helical Heat Exchangers Dimensions

Heat Exchanger	Tube/Sheet	d_i (mm)	d_o (mm)	t (mm)	D_c (mm)	H (mm)	L (mm)	N	P (mm)
½ inches heat exchanger	Hot Water Tube	11.08	12.7	0.81	235	177.8	5680	7	25.4
	Cold Water Tube	11.08	12.7	0.81	235	177.8	5680	7	25.4
	Thin Copper Sheet	-------	-------	0.2	234.6	177.8	740	1	------
5/8 inches heat exchanger	Hot Water Tube	14.26	15.88	0.81	235	222.32	5680	7	31.76
	Cold Water Tube	14.26	15.88	0.81	235	222.32	5680	7	31.76
	Thin Copper Sheet	-------	-------	0.2	234.6	222.32	740	1	-------

2.3 Meshing

Every part of the geometry was meshed separately with CFD physics preference and Fluent solver preference and adaptive size function. Edge sizing was applied on the circular faces of the fluid and solid parts for both cold and hot tubes with 25 divisions for each circle. The meshing method was automatic with medium smoothing. For ½ inches model, the total nodes number for the whole geometry was 1084474 nodes with equaled nodes number for solid pipes parts (217950 nodes for each part) and for fluid parts (126850 nodes for each part). The thin sheet solid part has 394874 nodes. For 5/8 inches model, the total nodes number for the whole geometry was the total nodes number for the whole geometry was 1114220nodes with equaled nodes number for solid pipes parts (208988 nodes for each part) and for fluid parts (101050 nodes for each part). The thin sheet solid part has 494144 nodes.

Figure (2) Mesh

2.4 Named Selection

The parts of the geometry was named as classified below:

1. Inlets and outlets: which define the hot and cold fluids entries and exits into and from the heat exchanger pipes.
2. Hot and cold fluids interfaces: which define the fluids inside the hot and cold pipes of the heat exchanger.
3. Interior and exterior walls interfaces: which define the solid walls of hot and cold pipes of the heat exchanger.

So, the parts names were:

1. Hot Fluid Inlet.
2. Cold Fluid Inlet.
3. Hot Fluid Outlet.
4. Cold Fluid Outlet.
5. Hot Fluid Interface-1.
6. Cold Fluid Interface-2.
7. Hot Interior Wall Interface-3.
8. Hot Exterior Wall Interface-4.
9. Cold Interior Wall Interface-5.
10. Cold Exterior Wall Interface-6.
11. Metal Sheet Slice interface-7.

The parts which involved in a heat transfer process were named with the word (interface), this will be used in (mesh interfaces menu) which is available in (set up window). The mesh interface between interfaces 1 and 3 defines heat transfer between hot fluid and hot interior wall. The mesh interface between interfaces 2 and 5 defines the heat transfer between cold fluid and cold interior wall. Finally, the mesh interface between interfaces 4, 6 and 7 defines heat transfer between hot exterior wall and cold exterior wall and the metal sheet slice.

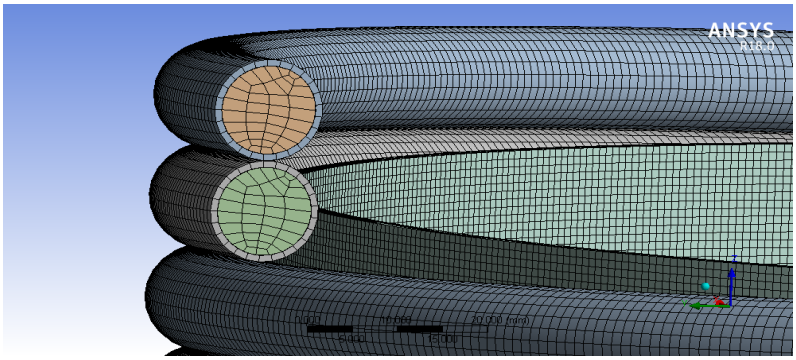

Figure (3) Close View of the Meshed Parts

Before starting calculations, set up window is used to complete setting up the problem. Energy model is set on and laminar viscous model is selected. Gravity is defined as z = - 9.81 m/s2. Calculation are run under steady state. Materials are chosen to be copper for solid parts and water for fluid parts. Boundary conditions are set for inlets, outlets, walls and other zones of the heat exchanger. Temperature difference is set to be 40 K(°C), where hot inlet temperature set as 328 K (55 C°) , and cold inlet temperature set as 288 K (15 C°). Mass flow rate for cold fluid inlet is varied from 0.5 to 1.5 LPM with 0.25 LPM step size. Hot fluid inlet is also varied from 0.5 to 1.5 LPM with each step of cold fluid inlet. 10,000 calculations are run to get results of outlet temperatures and many other parameters with their contours, vectors and plots.

3. Results and Discussions

3.1 Pressure Contours

Figure (4) shows the pressure variation through the heat exchanger. Obviously, both hot and cold water have a pressure drop between inlet and outlet. Figure (5: A and B) illustrates pressure variation in each hot water pipe and cold water pipe separately. Figure (5.A) demonstrates that the maximum pressure is at the top part of the exchanger (hot water inlet) and start decreasing until reach the minimum pressure at the bottom of the exchanger (hot water outlet). At the other side, figure (5.B) illustrates that the maximum pressure is at the bottom part of the exchanger (cold water inlet) and start decrease until reach the minimum pressure at the top part of the exchanger (cold water outlet).

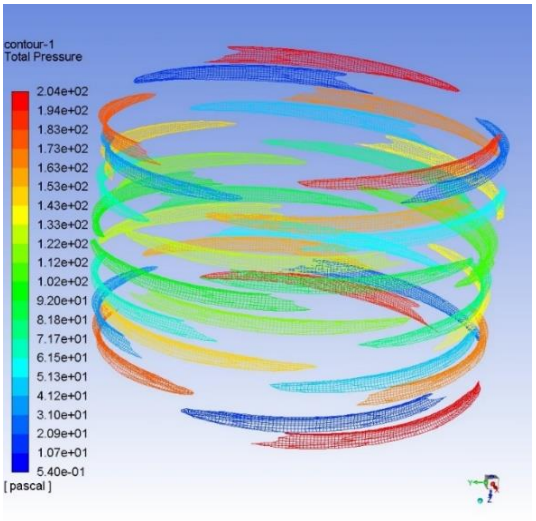

Figure (4) Pressure Contours of ½ inches H.E. at $Q_h = Q_c = 0.5$ LPM

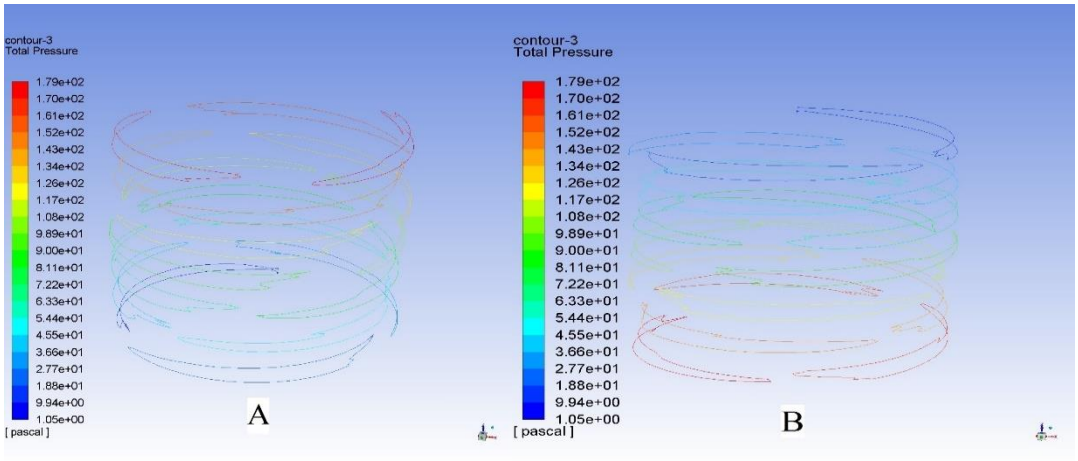

Figure (5) Pressure Contours of ½ inches H.E. at $Q_h = Q_c = 0.5$ LPM of (A) Hot Water Pipe, (B) Cold Water Pipe

3.2 Pressure drop

Figures (6) and (7) demonstrate pressure drop for cold and hot water for both ½ and 5/8 inches diameter heat exchangers, respectively. For both cold and hot water, pressure drop increases linearly with increasing hot and cold water flow rates, respectively. The maximum value was when applying 1.5 LPM cold or hot water, while the minimum value was when applying 0.5 LPM cold or hot water. It's can be noticed that the values of pressure drop of 0.5 inches heat exchanger are bigger than those of 5/8 inches heat exchanger because of the difference in diameter (pitch difference effect). Generally, the pressure drop accompanied to heat transfer process through the heat exchangers was very little amount which doesn't affect the cold or hot water pressure. The average value of maximum pressure (746 Pa) equals (0.00746 bar) which is considered a very slight pressure drop in industrial applications which utilize such heat exchangers.

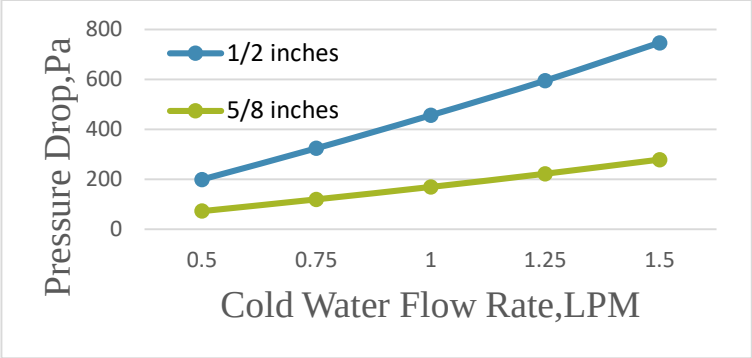

Figure (6) Cold Water Pressure Drop

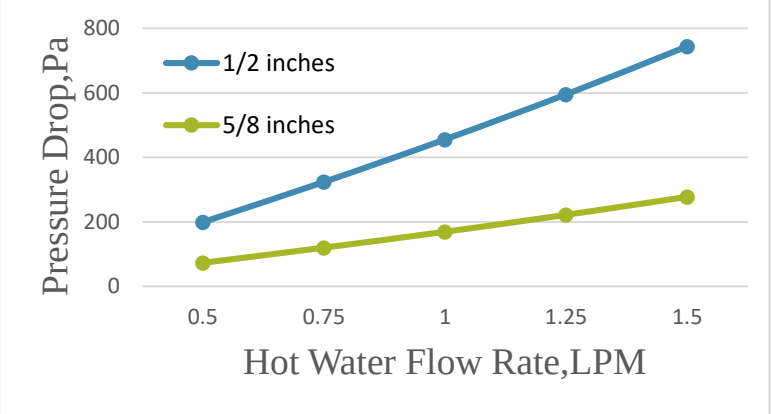

Figure (7) Hot Water Pressure Drop

3.3 Friction Factor

Figures (8) and (9) show friction factors values for both ½ and 5/8 inches diameter heat exchangers, respectively. Friction factor values can be computed from the following equations**(Wilson, 1915)**:

$$f_c = \frac{\Delta P}{(\frac{L_c}{d_{i\,c}})(\frac{\rho_c u_c^2}{2})} \quad \text{..... (5)}$$

$$f_h = \frac{\Delta P}{(\frac{L_h}{d_{i\,h}})(\frac{\rho_h u_h^2}{2})} \quad \text{..... (6)}$$

For cold and hot water, friction factor values decreases with increasing hot and cold water flowrates.The maximum value was when applying 0.5 LPM cold or hot water, while the minimum value was when applying 1.5 LPM cold or hot water.It's can be noticed that the values of friction factor of 5/8 inches heat exchanger are bigger than those of ½ inches heat exchanger because of the difference in diameter (pitch difference effect).

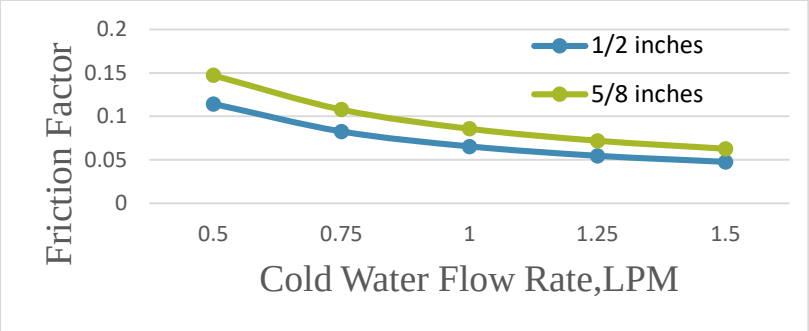

Figure (8) Cold Water Friction Factor

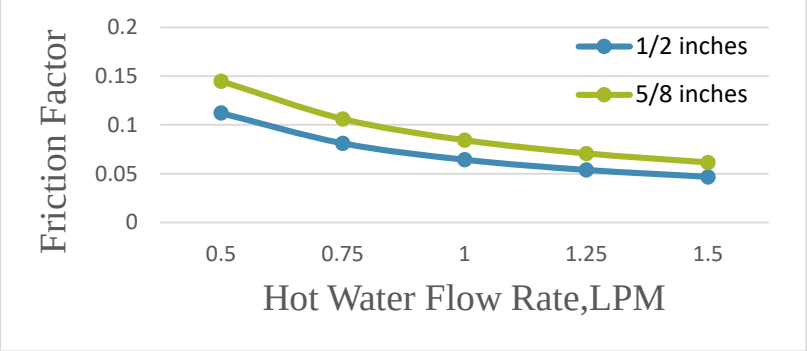

Figure (9) Hot Water Friction Factor

3.4Effectiveness & NTU

Heat exchanger effectiveness (ε) can be calculated from the equation below **(Wilson 1915)**:

$$\varepsilon = \frac{actual\ heat\ transfer\ in\ a\ heat\ exchanger}{maximum\ possible\ heat\ transfer\ in\ a\ heat\ exchanger} = \frac{q}{C_{min}(T_{hi}-T_{ci})} \quad \ldots\ldots\ldots (7)$$

Where actual heat can be taken as average heat which is calculated as:

$$q_{ave} = \frac{q_h+q_c}{2} \quad \ldots\ldots\ldots\ldots (8)$$

While the net heat transfer units (NTU) can be calculated from the equation **(Wilson, 1915)**:

$$NTU = \frac{UAs}{C_{min}} \quad \ldots\ldots\ldots\ldots (9)$$

The variations of effectiveness and NTU with different values of cold and hot water flow rates which are varied between (0.5-1.5) LPM are shown in figure (9) and (10) respectively for both 0.5 and 5/8 inches diameter heat exchangers. The minimum value was when applying 1.5 LPM for both cold and hot water, while the maximum value was when applying 1.5 LPM of hot water with 0.5 LPM of cold water. From the mentioned figures, it can be noticed that the increasing cold water flow rates causes increasing for both effectiveness and NTU for 0.5 LPM hot water flow rate. The other hot water flow rates start with high values of effectiveness and NTU at 0.5 LPM cold water and decreasing with increasing cold water flowrates and then increasing with increasing cold water flow rates. The 1.5 LPM hot water have a continuous decreasing in effectiveness and NTU with increasing hot water flow rates because of large amount of heat accompanied to 1.5 LPM hot water. Generally, the values of effectiveness and NTU are bigger in 0.5 inches diameter heat exchanger than those of 5/8 inches diameter heat exchanger.

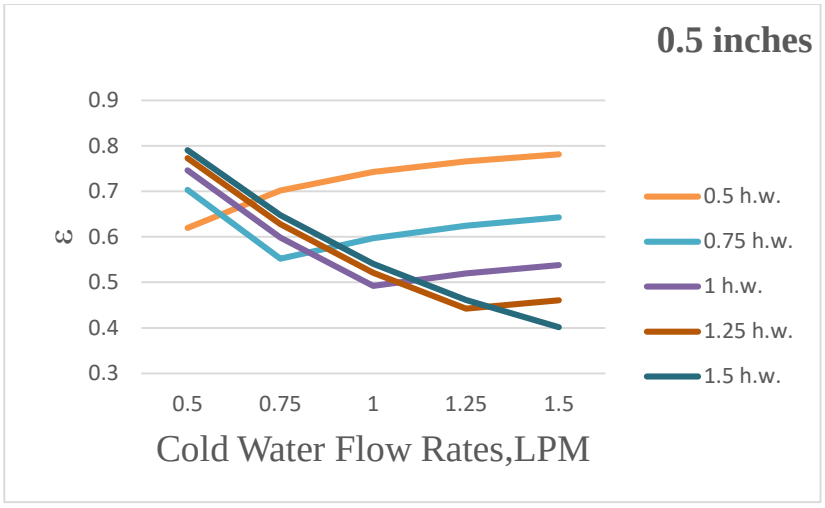

Figure (9-A) Effectiveness

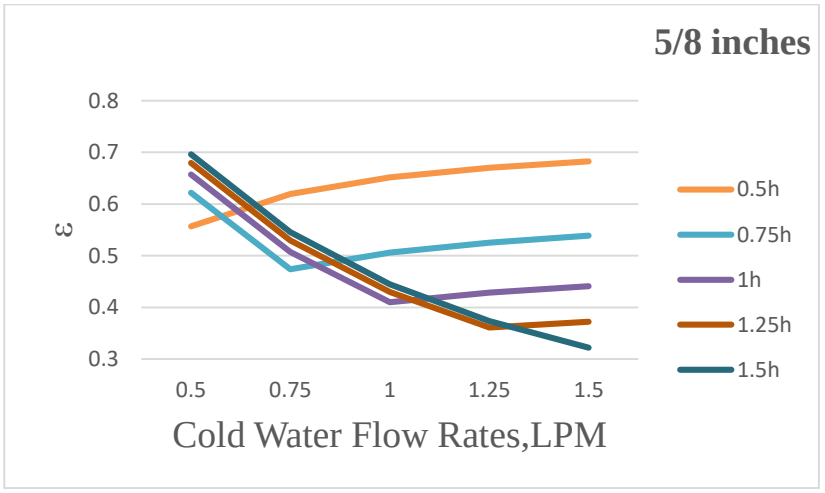

Figure (9-B) Effectiveness

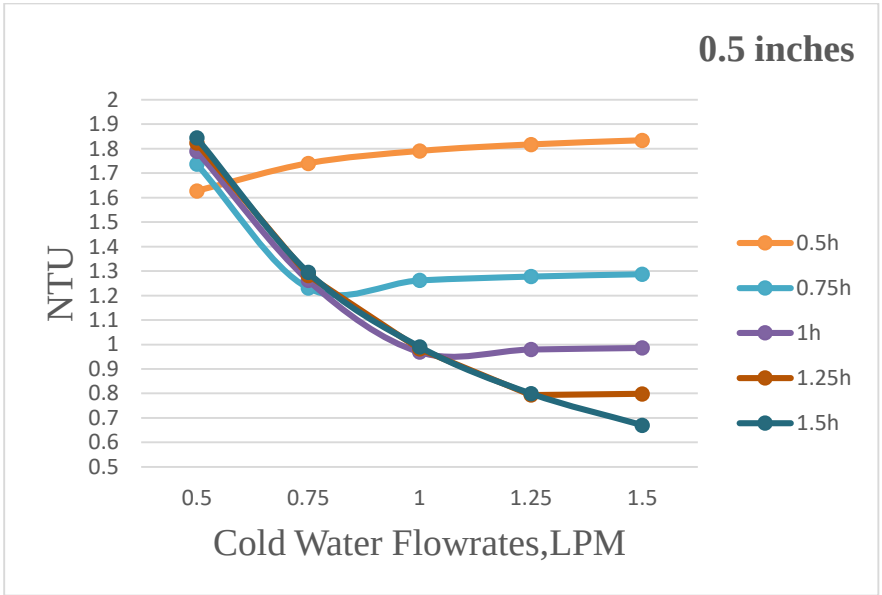

Figure (10-A) NTU

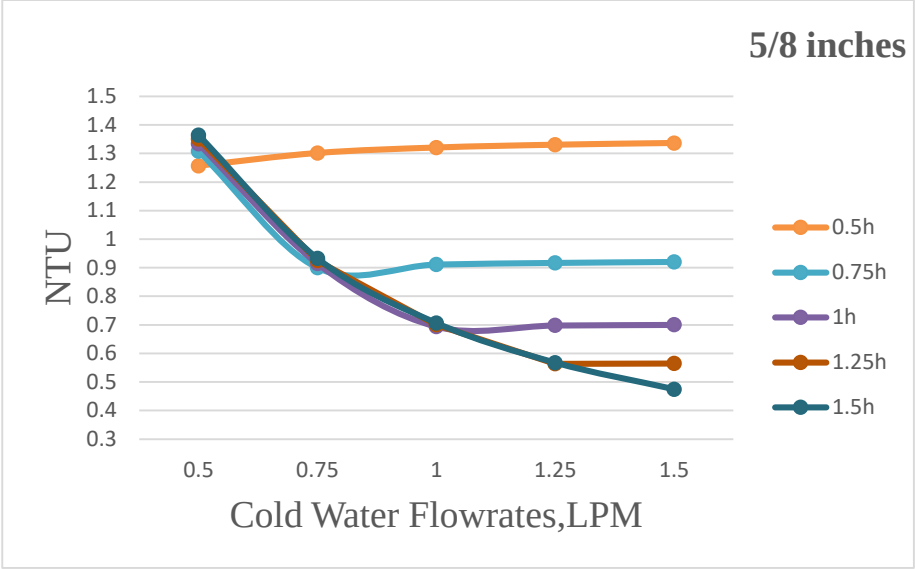

Figure (10-B) NTU

3.5Temperature Distribution

Figure (11: A and B) demonstrate static temperature contours for solid and fluid parts of the heat exchanger, respectively,whilefigure (12: A and B)demonstrates the static temperature for hot and cold pipes separately. In both figures, it can be noticed that the temperature increases or decreased gradually through the heat exchanger. Figure (13: A and B) shows the inlet hot and the outlet cold water static temperature contours. The figure demonstrates that the maximum hot inlet fluid temperature (328 k = 55 °C) occupies large area from the hot water inlet and starts to decrease near the solid walls. While in the cold outlet, the temperature is hotter near the solid walls and start to decrease until reaches (313 k = 40 °C) at the center of the cold outlet. Figure (13) clarifies also the graduation of static temperature between the solid walls and the fluid in both cold inlet and hot outlet.Figure (14) shows the static temperature contour of the metal sheet. This figure illustrate that the temperature decreases gradually from the top to the bottom.

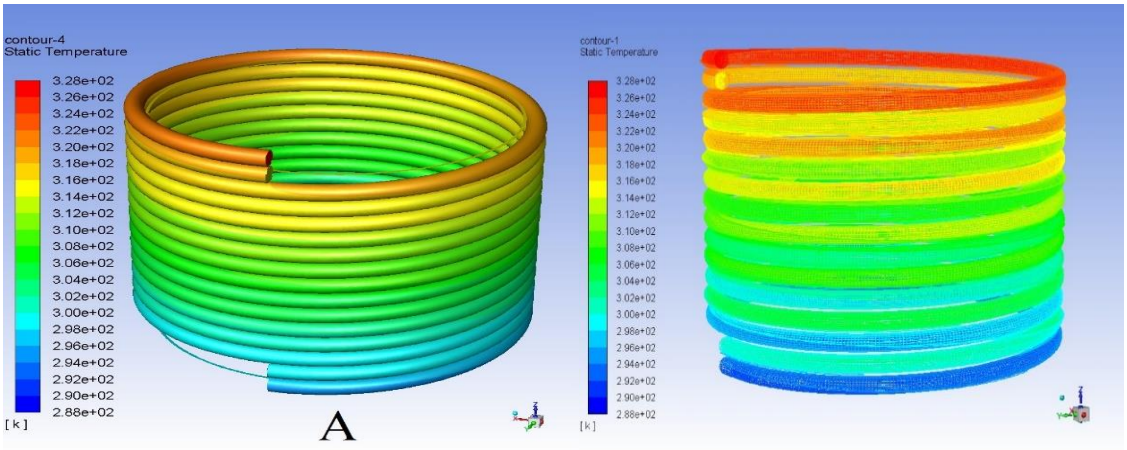

Figure (11) Static Temperature Contours for (A)Solid Parts (B) Fluid Parts of ½ inches H.E. at $Q_h = Q_c = 0.5$ LPM

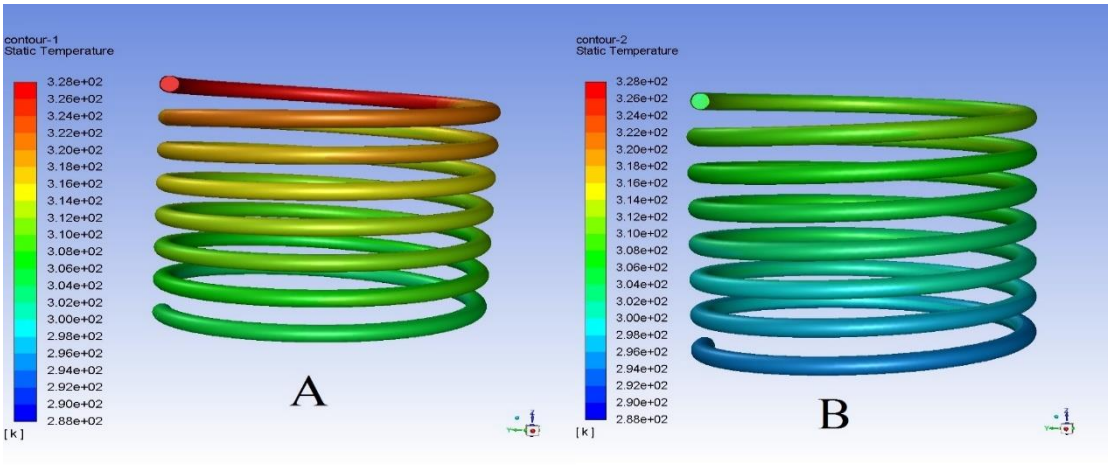

Figure (12) Static Temperature Contours for (A) Hot Water Pipe,
(B) Cold Water Pipe of ½ inches H.E. at $Q_h = Q_c = 0.5$ LPM

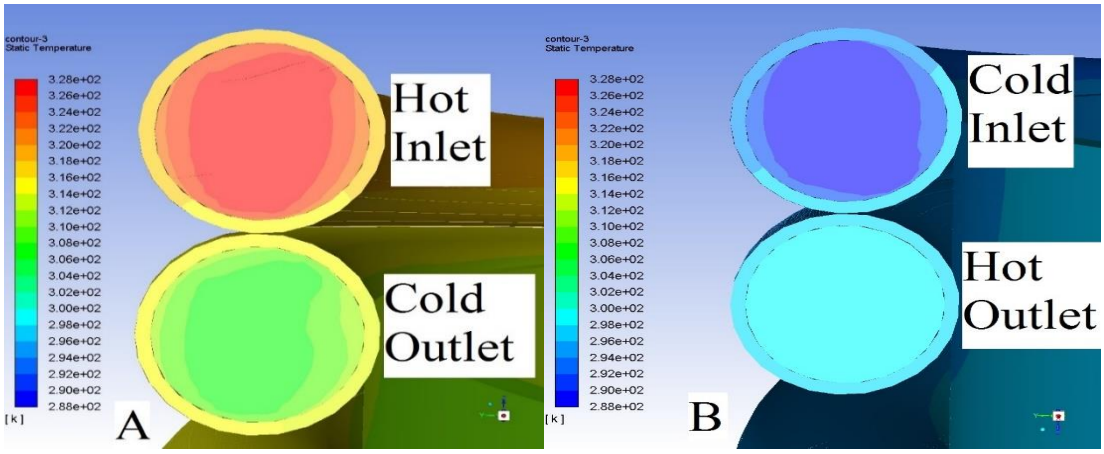

Figure (13) Static Temperature Contours in ½ inches H.E. at $Q_h = Q_c = 0.5$ LPM for (A) Hot Inlet and Cold Outlet,(B) Cold Inlet and Hot Outlet

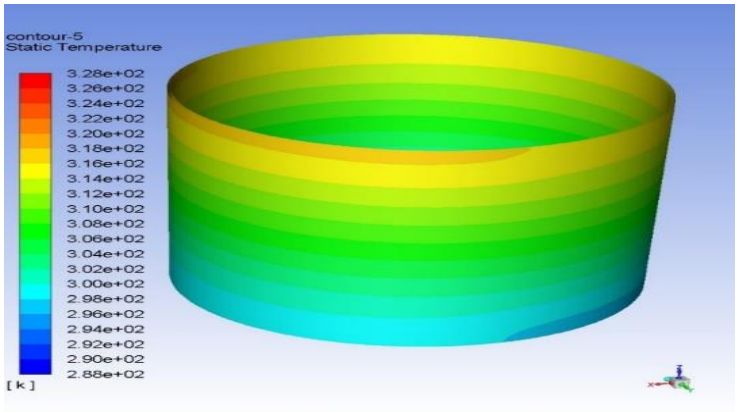

Figure (14) Static Temperature Contour of Metal (copper) Sheet of ½ inches H.E. at $Q_h = Q_c = 0.5$ LPM

3.6Velocity Contours

Figure (15) shows velocity contour for fluid parts of heat exchanger. It clarifies that the fluid tends to be static near the solid walls. The velocity of the fluid is concentrated in the center of the pipes as appears from the mentioned figure at the faces of the pipes. Figures (16: A and B) demonstrate the velocity magnitudes for both cold and hot water at inlets and outlets, which depend on the mass flow rate of the cold

and hot water. The maximum velocity was 0.26 m/s when applying 1.5 LPM of hot water, while the minimum velocity was 0.086 m/s when applying 0.5 LPM of cold water.

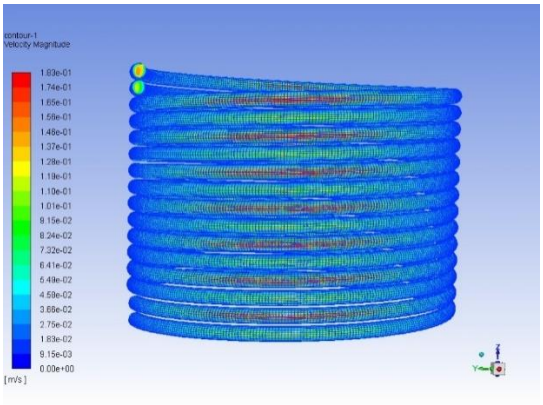

Figure (15) Velocity Magnitude Contour for Fluid Parts

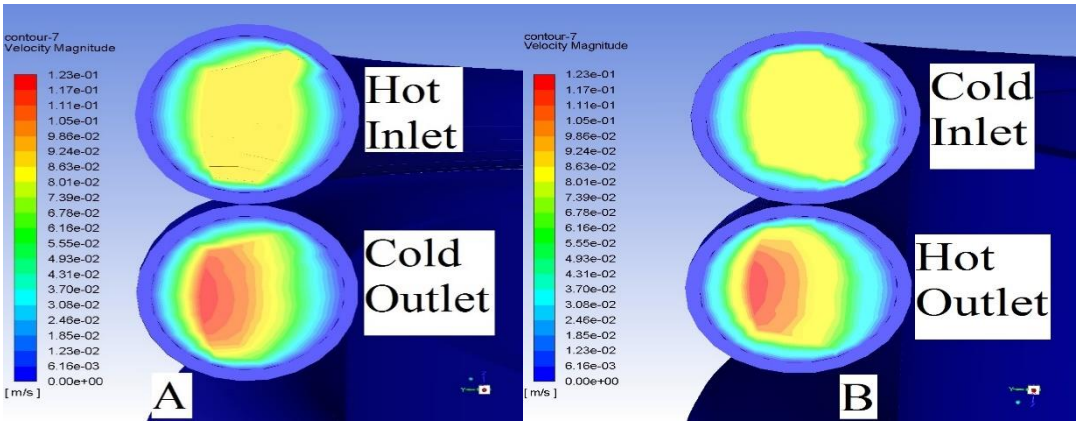

Figure (16) Velocity Magnitude Contour of ½ inches H.E. at $Q_h = Q_c = 0.5$ LPM for (A) Hot Inlet and Cold Outlet, (B) Cold Inlet and Hot Outlet

4. Conclusions

The present paper, analyses a CFD simulation for heat transfer enhancement in an interfered double helical heat exchanger which utilizes the passive effect of the secondary flow generated from the helical (curved) pipes manufacturing the heat exchanger. The key findings are as mentioned below:

1. The pressure drop is increased linearly for both cold and hot water in both 0.5 and 5/8 inches diameter heat exchangers.
2. The maximum pressure drop is approximately 746 Pa, while the minimum pressure drop is approximately 199 Pa for 0.5 inches diameter H.E., while 5/8 inches diameter H.E. ha a maximum and minimum pressure drop of approximately 278 Pa and 72 Pa respectively. Maximum pressure drop represents 0.746 % of 1 bar which is very small amount and doesn't affect the cold or hot water pressure.
3. The effectiveness value is increased when applying small amount of hot water with increasing the cold water flowrates which increases the intensity of the secondary flow. Secondary flow is considered as an important heat transfer enhancement passive technique which is used in the simulation in this paper.
4. For 0.5 inches diameter H.E., The maximum effectiveness value is 0.79 when applying 0.5 LPM cold water with 1.5 LPM hot water, while the minimum effectiveness value is 0.401 when applying 1.5 LPM hot water with 1.5 LPM cold water.

5. For 5/8 inches diameter H.E., The maximum effectiveness value is 0.696 when applying 0.5 LPM cold water with 1.5 LPM hot water, while the minimum effectiveness value is 0.322 when applying 1.5 LPM hot water with 1.5 LPM cold water.
6. Pitch decreasing from 31.756 mm to 25.4 mm causes effectiveness increasing by approximately 15%.
7. The NTU value is increased when applying small amount of hot water with increasing the cold water flowrates which increases the intensity of the secondary flow.
8. For 0.5 inches diameter H.E., The maximum NTU value is 1.84 when applying 0.5 LPM cold water with 1.5 LPM hot water, while the minimum NTU value is 0.66 when applying 1.5 LPM hot water with 1.5 LPM cold water.
9. For 5/8 inches diameter H.E., The maximum NTU value is 1.36 when applying 0.5 LPM cold water with 1.5 LPM hot water, while the minimum NTU value is 0.47 when applying 1.5 LPM hot water with 1.5 LPM cold water.
10. Pitch decreasing from 31.756 mm to 25.4 mm causes NTU increasing by approximately 35%.

References

1. Baqir, A. S., Mahood, H. B. and Kareem, A. R. (2019) 'Optimisation and Evaluation of NTU and Effectiveness of a Helical Coil Tube Heat Exchanger with Air Injection', Thermal Science and Engineering Progress, 14(May), p. 100420. doi: 10.1016/j.tsep.2019.100420
2. Barua, S. N. "On Secondary Flow in Stationary Curved Pipes", Quarterly Journal of Mechanics and Applied Mathematics, 16(1), pp. 61–77. doi: 10.1093/qjmam/16.1.61., (1963)
3. Bergles, A. E., Jensen, M. K. and Shome, B. "The Literature on Enhancement of Convective Heat and Mass Transfer", Journal of Enhanced Heat Transfer, 4(1), pp. 1–6., (1996)
4. Bizhaem, H. K. and Abbassi, A. "Numerical Study on Heat Transfer and Entropy Generation of Developing Laminar Nanofluid Flow in Helical Tube Using Two-Phase Mixture Model", Advanced Powder Technology, 28(9), pp. 2110–2125. doi: 10.1016/j.apt.2017.05.018., (2017)
5. Datta, A. K. et al. "Laminar Forced Convective Heat Transfer in Helical Pipe Flow", International Journal of Thermal Sciences, 120, pp. 41–49. doi: 10.1016/j.ijthermalsci.2017.05.026., (2017)
6. Day, J.,"Laminar Natural Convection from Isothermal Vertical Cylinders" Master of Science, University of North Texas, August(2012).
7. Ghashim, S. L. and Flayh, A. M. "Experimental Investigation of Heat Transfer Enhancement in Heat Exchanger due to Air Bubbles Injection", Journal of King Saud University - Engineering Sciences, (xxxx), pp. 0–7. doi: 10.1016/j.jksues.2020.06.006., (2020)
8. Ghobadi, M. "Experimental Measurement and Modelling of Heat Transfer in Spiral and Curved Channels", Memorial University of Newfoundland May, (2014)
9. Kong, R. et al. "Heat Transfer Phenomena on Waste Heat Recovery of Combustion Stack Gas with Deionized Water in Helical Coiled Heat Exchanger", Case Studies in Thermal Engineering, 12, pp. 213–222. doi: 10.1016/j.csite.2018.04.010., (2018)
10. Mohanty, S. R. "CFD Analysis of Heat Transfer in a Helical Coil Heat Exchanger Using Fluent",Department of Mechanical Engineering National Institute of Technology Rourkela 769008., (2013)

11. Sharifi, K. et al. ‘Computational Fluid Dynamics (CFD) Technique to Study The Effects of Helical Wire Inserts on Heat Transfer and Pressure Drop in a Double Pipe Heat Exchanger’, Applied Thermal Engineering, 128, pp. 898–910. doi: 10.1016/j.applthermaleng.2017.08.146.,(2018)
12. Shatat, M. M. E. M. “Influence of Micro-Bubbles on The Heat Transfer and Pressure Drop Characteristics of Water Flow in Straight and Helical Pipes”,Okayama:Okayama University, (2010)
13. Wilson, E. E. “A Basis for Rational Design of Heat Transfer Apparatus”, The J. Am. Soc. Mech. Engrs., 37, pp. 546–551., (1915)
14. Yang, G., Dong, Z. F. and Ebadian, M. A. “Laminar Forced Convection in a Helicoidal Pipe with Finite Pitch”, International Journal of Heat and Mass Transfer, 38(5), pp. 853–862. doi: 10.1016/0017-9310(94)00199-6., (1995)